

IR-Active Phonons and Structure Elements of Isotope-Enriched Boron Carbide

H. Werheit, T. Au, and R. Schmechel¹

Solid State Physics Laboratory, Gerhard-Mercator University of Duisburg, D-47048 Duisburg, Germany

and

S. O. Shalamberidze, G. I. Kalandadze, and A. M. Eristavi

Institute of Stable Isotopes, 21, Kavtaradze Street, Tbilisi, 380086, Georgia

Received September 9, 1999; in revised form December 28, 1999; accepted January 2, 2000

The IR phonon spectra of ¹⁰B, ¹¹B, and ¹³C isotope-enriched boron carbide with the compositions B_{4.3}C, B_{6.5}C, and B₁₀C are presented. Specific phonons are attributed to the stretching and the bending mode of a small concentration of CCC chains, whose occurrence seems to depend on the specific preparation conditions. Based on the assumption that the electron deficiency is compensated by structural defects, the concentrations of CBC, CBB, CCC, and B□B arrangements are determined for the whole homogeneity range. Then the concentrations of B₁₂ and B₁₁C icosahedra result from the compound stoichiometry. The concentration of B□B arrangements, calculated this way, excellently agrees with the concentration of B(3) vacancies obtained by neutron scattering. © 2000 Academic Press

INTRODUCTION

The electron densities of boron and carbon atoms are not sufficiently different to be resolved by the present possibilities of X-ray structure investigations; moreover the C atoms are partly statistically distributed on specific regular B sites. NMR failed to determine the real boron carbide structure as well. Theoretical calculations were based on idealized structures, which are not in agreement with realistic structures. The first information on the real composition of boron carbide unit cells throughout the homogeneity range was obtained from phonon spectroscopy by Kuhlmann *et al.* (1,2) More recently Schmechel and Werheit (3) proved that the electron deficiency theoretically calculated for the idealized B₁₂CBC structure, which was shown by Bylander

and Kleinman (4,5) to be the energetically most favorable one, is exactly compensated by the structural defects derived from phonon spectra (6,13). Thus, the theoretically resulting metallic character is changed to the experimentally proved semiconducting behavior. The same was shown to hold for the whole homogeneity range of boron carbide and for β-rhombohedral boron as well (3). Such structural defects are C atoms substituting for regular B sites and generating donors, B atoms substituting for regular C sites and generating acceptors, vacancies forming localized states in the band gap, and in particular vacancies in the structures.

These results underline the importance of phonon spectroscopy to understand the general properties of the icosahedral boron-rich solids. To convey a better insight into the lattice vibration spectrum of boron carbide, investigations on isotope-enriched material are presented below (for some details of sample properties see Table 1).

Earlier investigations of the phonon spectra of isotope-enriched boron carbide were performed by Kuhlmann and Werheit (IR absorption and Raman spectra of ¹⁰B_{4.3}C) (1,2,6), Stein *et al.* (IR reflectivity of bulk ¹¹B₄¹²C, ¹¹B₄¹³C, ¹¹B₉¹³C and IR transmission of KBr pellets of powdered ¹⁰B₄¹²C, ¹¹B₄¹²C) (7), and Aselage *et al.* (conventionally measured Raman spectra (with high excitation energy) of ¹¹B_{12.15}¹³C_{2.85}, ¹¹B_{12.15}¹²C_{2.85}, ¹⁰B_{12.15}¹²C_{2.85}, ¹¹B_{12.15}¹²C_{2.85}) (8). However, neither reflectivity spectra of bulk material nor transmission spectra of KBr pellets are suitable for determining phonon resonance frequencies with sufficiently high precision to reliably calculate isotope-dependent shifts, at least not without very careful analysis. Therefore it is not surprising that these results considerably deviate from those presented below. In contrast to FT Raman spectra, the conventional Raman spectra of boron carbide were shown to be strongly influenced by the surface properties of the

¹ Present address: Darmstadt University of Technology, Material Science, Department of Electronic Materials, D-64287 Darmstadt, Germany.



TABLE 1
Investigated Samples and Their Vickers Microhardness Measured with 200 g Load

^{11}B enriched		^{10}B enriched		^{10}B and ^{13}C enriched	
Compound	Microhardness [GPa]	Compound	Microhardness [GPa]	Compound	Microhardness [GPa]
$\text{B}_{4.3}\text{C}$	41	$\text{B}_{4.3}\text{C}$	43.8	$\text{B}_{4.3}\text{C}$	34
$\text{B}_{6.5}\text{C}$	43.8	$\text{B}_{6.5}\text{C}$	41	$\text{B}_{6.5}\text{C}$	49
B_{10}C	39	B_{10}C	42.5	B_{10}C	44

samples (9). Accordingly, it must be guessed that at least some of the measured Raman bands are to be attributed to chemical compounds at the surface.

SAMPLE MATERIAL

The sample material was prepared by hot-pressing at 40 MPa for 30 min at 2000–2050°C from powder obtained by a direct total synthesis of the elements (1950°C, 2 h). The isotope-enriched boron was obtained from KBF_4 by an electrolysis method. The isotope enrichment was 98.4 at.% ^{10}B , 99.4(2) at.% ^{11}B , and 80.1(2) at.% ^{13}C , respectively. Impurities are Fe (0.6 wt.%) and Mg, Si, Al, Ca, and Cu (in total 1.3 wt.%).

For the optical reflectivity measurements slices of about 1 mm thickness were cut from the specimens, and grinded and polished on rotating disks with diamond spray (Stuers) of decreasing grain size (final 1 μm) to minimize the thickness of Beilby layers.

OPTICAL SPECTRA

The reflectivity spectra were measured with a FTIR spectrometer (Bruker 113v) in the spectral range between 100 and 5000 cm^{-1} , resolution 2 cm^{-1} . The absorption spectra were calculated from the reflectivity spectra using the Kramers-Kronig relation. Figures 1a and 1b display the reflectivity and absorption spectra of the ^{10}B -enriched samples of different compositions between 200 and 2000 cm^{-1} . In Figs. 2a–2c the absorption spectra of the differently isotope-enriched samples with the same chemical composition are compared. In Table 2 the peak resonance frequencies, the relative oscillator strengths obtained by integrating the peak areas, and the half-widths of the peaks are listed.

DISCUSSION

According to group theory the phonon spectrum of boron carbide with the idealized structure consisting of one

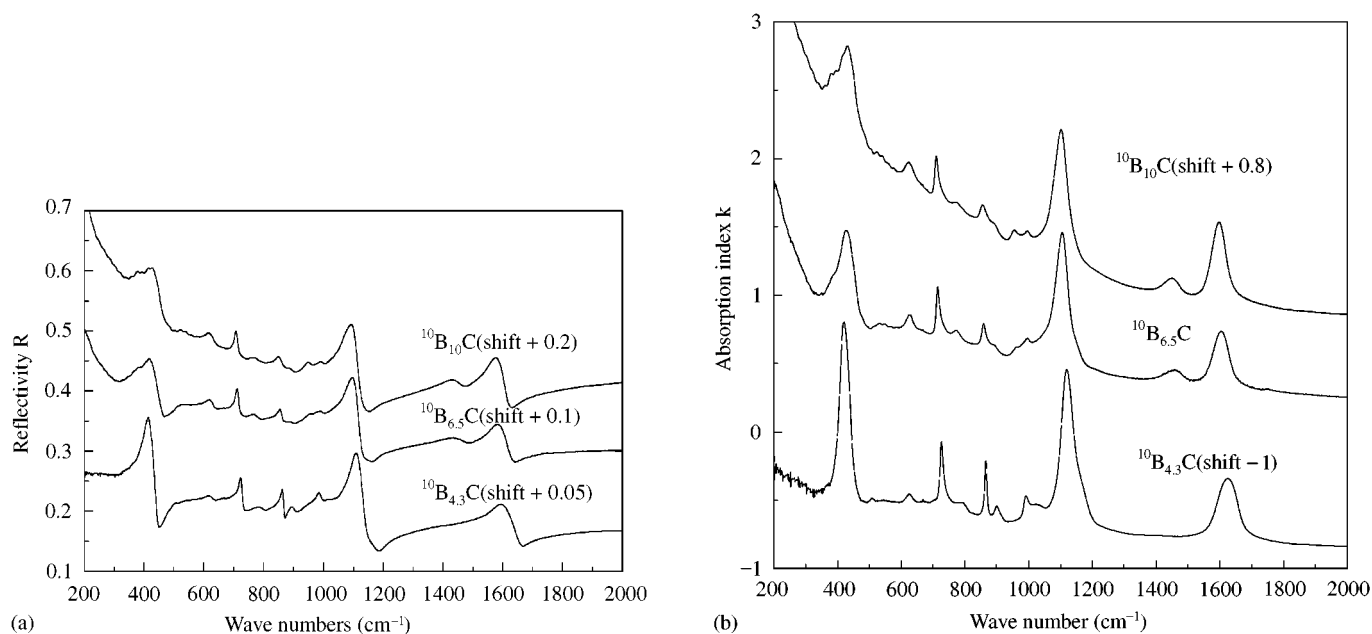


FIG. 1. (a) Reflectivity and (b) absorption index of ^{10}B -enriched boron carbide; compounds $\text{B}_{4.3}\text{C}$, $\text{B}_{6.5}\text{C}$, and B_{10}C .

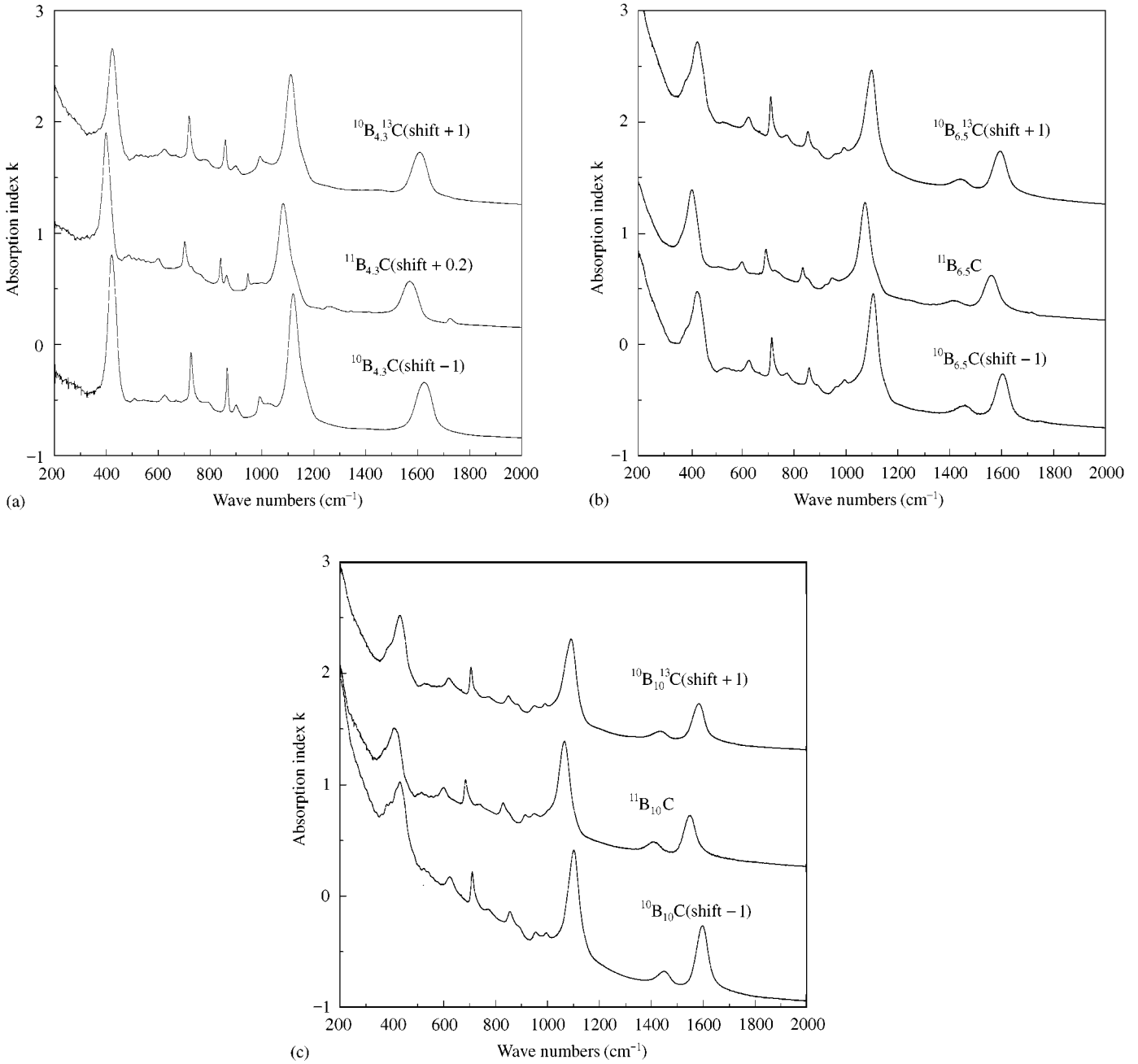


FIG. 2. Absorption coefficient of (a) B_{4.3}C, (b) B_{6.5}C, and (c) B₁₀C enriched with 10B, 11B and 10B + 13C isotopes, respectively.

icosahedron and a three-atom chain on the trigonal axis exhibits 8 IR-active modes (5 A_{2u} $E \parallel c$ (+1 translation) and 5 E_u $E \perp c$) and 11 Raman active modes (5 A_{1g} $E \parallel c$ and 6 E_g $E \perp c$ (+1 rotation) (10, 11). For idealized B₁₃C₂ with complete D_{3d} symmetry there are 12 IR-active and 12 Raman-active modes (12). Since the real structure of boron carbide consists of mixtures of different structural elements (at least B₁₂ and B₁₁C icosahedra, CBC and CBB chains, and chainless unit cells), the real number of phonons is expected to be higher than that, which is group theoretically

expected. In Table 3 the phonons determined for isotope-enriched boron carbide (Table 2) are attributed to the symmetry types based on experimental results (6) (see also (13)) and theoretical calculations (12).

In the phonon spectrum of boron carbide the vibrations of the chain and of the icosahedron can be distinguished. For B_{4.3}C the band at 1620 cm⁻¹ was attributed to the stretching mode and the band at 410 cm⁻¹ essentially to the bending mode of the linear three-atom chain, while the other phonons are intraicosahedral vibrations (6, 1, 2).

TABLE 2
Resonance Frequencies $\tilde{\nu}$ in cm^{-1} , Relative Oscillator Strengths (Integrated Area of the Peaks), and Half-Widths of Phonons in Isotope-Enriched Boron Carbides

No.	$^{10}\text{B}_{4,3}\text{C}$			$^{11}\text{B}_{4,3}\text{C}$			$^{10}\text{B}_{4,3}\text{ }^{13}\text{C}$		
	$\tilde{\nu}$	A	$B_{1/2}$	$\tilde{\nu}$	A	$B_{1/2}$	$\tilde{\nu}$	A	$B_{1/2}$
1	—	—	—	—	—	—	—	—	—
2	421	48.3	36.2	399	36.4	33.8	423	34.2	37.6
3	510	0.4	13.5	487	0.8	22.9	(515)	—	—
4	625	1.3	22.4	601	1.0	21.5	624	1.5	24.6
5	668	—	—	668	—	—	668	—	—
6	727	6.5	12.4	702	3.2	12.6	719	5.9	12.7
7	(789)	—	—	—	—	—	(778)	—	—
8	866	3.9	8.2	841	1.9	8.2	858	3.3	10.8
9	900	1.5	18.3	863	1.1	13.0	898	1.1	21.9
10	992	0.7	11.1	946	0.9	7.1	992	1.4	19.5
11	(1023)	0.3	—	(998)	0.1	15.2	(1018)	—	—
12	1120	58.1	45.7	1081	44.6	49.4	1111	46.3	45.1
13	—	—	—	1252	1.1	37.5	—	—	—
14	—	—	—	—	—	—	—	—	—
15	1624	32.7	71.5	1568	24.3	67.8	1609	27.0	67.9
16	—	—	—	1722	0.9	21.5	—	—	—
No.	$^{10}\text{B}_{6,5}\text{C}$			$^{11}\text{B}_{6,5}\text{C}$			$^{10}\text{B}_{6,5}\text{ }^{13}\text{C}$		
	$\tilde{\nu}$	A	$B_{1/2}$	$\tilde{\nu}$	A	$B_{1/2}$	$\tilde{\nu}$	A	$B_{1/2}$
1	(386)	—	—	(366)	—	—	(387)	—	—
2	427	34.4	57.1	407	31.3	49.3	429	36.7	59.9
3	537	1.0	34.2	(508)	—	—	(534)	—	—
4	626	2.5	23.5	600	1.9	21.6	625	2.8	25.3
5	668	—	—	668	—	—	668	—	—
6	715	5.6	12.8	692	3.5	15.0	711	5.7	12.4
7	(774)	—	—	(739)	—	—	772	—	—
8	859	2.5	14.1	834	2.4	17.7	854	2.5	15.6
9	(890)	—	—	(853)	—	—	(885)	—	—
10	(962)	—	—	(923)	—	—	(960)	—	—
11	(995)	0.8	17.7	(947)	0.9	25	(993)	0.6	15.6
12	1105	47.5	45.1	1074	40.8	46.6	1099	46.5	49.8
13	—	—	—	—	—	—	—	—	—
14	1458	4.5	62.4	1411	2.6	62.8	1440	4.0	63.9
15	1604	22.7	55.5	1558	19.0	60.7	1594	23.8	61.5
16	(1752)	—	—	1717	0.2	—	—	—	—
No.	$^{10}\text{B}_{10}\text{C}$			$^{11}\text{B}_{10}\text{C}$			$^{10}\text{B}_{10}\text{ }^{13}\text{C}$		
	$\tilde{\nu}$	A	$B_{1/2}$	$\tilde{\nu}$	A	$B_{1/2}$	$\tilde{\nu}$	A	$B_{1/2}$
1	(390)	—	—	(372)	—	—	(388)	—	—
2	431	35.5	81.5	410	26.5	72.6	432	31.3	59.2
3	(524)	—	—	514	1.0	27.7	(528)	—	—
4	624	2.4	26.8	600	2.2	25.0	620	2.4	26.9
5	668	—	—	668	—	—	668	—	—
6	710	4.9	13.8	684	3.8	14.4	706	4.1	12.3
7	(772)	—	—	(736)	—	—	(773)	—	—
8	856	2.3	20.8	829	3.7	26.4	850	3.2	31.6
9	(887)	—	—	(848)	—	—	(883)	—	—
10	955	—	—	914	—	—	950	—	—
11	996	0.5	14.0	(949)	0.5	21.8	990	0.3	12.5
12	1102	49.0	49.6	1065	43.3	48.5	1091	39.6	53.7
13	—	—	—	—	—	—	—	—	—
14	1448	5.3	54.0	1406	4.4	55.4	1436	3.3	56.5
15	1597	32.0	51.9	1550	19.2	51.6	1584	20.2	53.3
16	—	—	—	—	—	—	—	—	—

Note. Uncertain values are in parentheses.

TABLE 3
Attribution of the Lattice Vibrations to the Symmetry Types Experimentally Determined by Kuhlmann (6) and Theoretically Calculated by Shirai and Emura (8)

No.	This work	Kuhlmann, exp. (6)		Shirai and Emura, theor. (12)	
	$^{11}\text{B}_{6,5}\text{C}$ Wave number (cm^{-1})	$^{\text{nat}}\text{B}_{6,3}\text{C}$ Wave number (cm^{-1})	$^{10}\text{B}_{4,3}\text{C}$ Symmetry type	$\text{B}_{6,5}\text{C}$ Wave number (cm^{-1})	Symmetry type
	—	72	—	—	—
	—	110	—	—	—
	—	195	—	—	—
	—	274	—	268	A_{2u}
	—	329	—	314	E_u
	—	378	—	393	E_u
1	407	410.3	$A_{2u} + E_u$	434	E_u
	—	429	—	—	—
2	508	515	—	487	E_u
3	600	—	—	—	—
4	668	606	E_u	673	A_{2u}
	—	665	—	—	—
5	692	696	E_u	690	E_u
6	739	752	(E_u)	738	A_{2u}
7	834	838.7	E_u	748	E_u
8	853	865.5	A_{2u}	—	—
9	923	929.4	A_{2u}	—	—
10	947	962	A_{2u}	—	—
	—	1014	(A_{2u})	—	—
11	1074	1081	E_u	1041	E_u
12	—	—	—	—	—
13	1411	1427	—	—	—
14	1558	1580	A_{2u}	1575	A_{2u}

The vibrations of the chain can be discussed in analogy to the vibrations of linear two-atomic molecules (14). After Waser and Pauling (15) the Badger rule of the relation between force constants and interatomic distances in diatomic molecules (16) holds for solids as well. Hence for B and C belonging to the same row in the periodic table, universal interaction constants can be expected. For some boron-rich solids this was already checked in (17). The stretching mode is the antiphase vibration between the central atom and the end atoms of the three-atom chain, which for $\text{B}_{4,3}\text{C}$ essentially consists of CBC arrangements. For $^{10}\text{B} \rightarrow ^{11}\text{B}$ the phonon frequency shifts to lower values, while it surprisingly remains largely unchanged for $^{12}\text{C} \rightarrow ^{13}\text{C}$. Accordingly, the vibration is essentially determined by the central B atom of the chain and its shift by the mass relation, and can approximately be described by $\omega = \sqrt{k/m(B)}$. The accordingly expected frequency shift

$$\omega(^{10}\text{B})/\omega(^{11}\text{B}) = \sqrt{m(^{11}\text{B})/m(^{10}\text{B})} = 1.048$$

well agrees with the experimentally determined frequency relation of the stretching mode

$$\omega_s(^{10}\text{B})/\omega_s(^{11}\text{B}) = 1624/1568 = 1.036,$$

and of the bending mode

$$\omega_b(^{10}\text{B})/\omega_b(^{11}\text{B}) = 421/399 = 1.035$$

as well.

The relation for the stretching mode of the three-atom chain (14)

$$\omega^2 = (1 + 2m_y/m_x) \cdot k/m_y$$

makes it possible to estimate the force constants k , which well agree with experimental results (1, 2, 6) and theoretical calculations (12, 18) of other authors (Table 4). Indeed, there is a certain inconsistency between this equation and the experimental fact that the resonance frequency does not essentially depend on the mass of the terminal atoms of the chain.

It is not surprising that the theoretical results best agree with the experimental results for $^{11}\text{B}_{6,5}^{12}\text{C}$, because this compound is closest to the model composition used for the theoretical calculations.

Significant peculiarity in the spectra of the boron-rich boron carbides are specific phonons at $\omega_{s1} \approx 1400$ to 1600 cm^{-1} (No. 14 in Table 2), which are comparable for all

TABLE 4
Force Constants k (mdyn \AA^{-1}) of the Three-Atom Chain (Composition-Dependent Mixtures of CBC and CBB)

Compound	k (this work)	k average	k (exp) Kuhlmann <i>et al.</i> (1,2,6)	k (theor.) Abbot and Beckel (18)	k (theor.) Shirai and Emura (8)
$^{10}\text{B}_{4.3}^{12}\text{C}$	5.53				
$^{11}\text{B}_{4.3}^{12}\text{C}$	5.51	5.53	5.56		
$^{10}\text{B}_{4.3}^{13}\text{C}$	5.55				
$^{10}\text{B}_{6.5}^{12}\text{C}$	5.39				
$^{11}\text{B}_{6.5}^{12}\text{C}$	5.44	5.43	5.52	5.4/5.38	5.4
$^{10}\text{B}_{6.5}^{13}\text{C}$	5.45				
$^{10}\text{B}_{10}^{12}\text{C}$	5.35				
$^{11}\text{B}_{10}^{12}\text{C}$	5.38	5.37	5.18		
$^{10}\text{B}_{10}^{13}\text{C}$	5.38				

$\text{B}_{6.5}\text{C}$ and B_{10}C samples and obviously correlated with the low-frequency phonons at $\omega_{\text{bl}} \approx 380 \text{ cm}^{-1}$ (No. 1 in Table 2). Both bands are slightly shifted toward frequencies lower than the main resonance frequencies of the chain. In agreement with the spectra obtained formerly this additional phonon does not occur in the $\text{B}_{4.3}\text{C}$ compounds. Since its appearance in the former spectra of boron-rich boron carbides was only arbitrary, it has not yet been considered in the discussions of phonon spectra. The shift of the phonon frequencies

$$\omega_{\text{s}}(^{10}\text{B})/\omega_{\text{sl}}(^{10}\text{B}) \approx \omega_{\text{s}}(^{11}\text{B})/\omega_{\text{sl}}(^{11}\text{B}) \approx 1.114(26)$$

$$\omega_{\text{s}}(^{10}\text{B}^{13}\text{C})/\omega_{\text{sl}}(^{10}\text{B}^{13}\text{C}) \approx 1.105(2)$$

can be well described by the relation

$$\omega(^{10(11)}\text{B})/\omega(^{12(13)}\text{C}) = \sqrt{m(^{12(13)}\text{C})/m(^{10(11)}\text{B})} = 1.092.$$

This leads to the conclusion that the phonon is due to a chain with a central C atom, probably BCB or CCC. The frequency shift of the phonon depending on the different isotopes is weak (Table 2); nevertheless it is measurable for the change of the B isotope and of the C isotope as well. This seems to support the BCB arrangement.

In Table 5 the force constants calculated for CCC and CBC arrangements are listed. Again the values for $^{11}\text{B}_{6.5}^{12}\text{C}$ are the most relevant because they are based on the atomic distances for this compound. The results for the CCC chain model are distinctly closer to those determined for the main chains. This favors the CCC arrangement for the additional chain.

A further way to check the kind of additional chain, BCB or CCC, is based on the determination of the electron deficiency of the compounds in the boron carbide homogeneity range compared with the idealized structure B_{12}CBC shown by Bylander and Kleinman (4) to be the energetically most favorable. Schmechel and Werheit (3) have proved that

in the real structure this electron deficiency is compensated by the generation of structural defects in the form of B_{11}C icosahedra, CBB chains, and $\text{B}\square\text{B}$ arrangements (\square , vacancy). Electronically, each substitution of a C atom for a regular B atom is assumed to evoke a donor state without influence on the valence band density of states, and each substitution $\text{B} \rightarrow \text{C}$ an acceptor state splitting one state from the valence band; from the two broken bonds in each $\text{B}(3)$ vacancy ($\text{B}(3)$, central chain atom) two localized states are expected to split from the valence band (for details see (3)). The concentration of $\text{B}\square\text{B}$ arrangements calculated accordingly can be checked by the concentration of the $\text{B}(3)$ vacancies determined by neutron diffraction (19).

The calculation is based on the following equations modified in comparison to those in (3), where the phonon band ω_{sl} was ignored because its appearance in the boron carbide samples investigated previously was only accidental.

For the attribution of BCB arrangements to the separated chain phonon one gets the following conditions:

(i) The electron deficiency D is compensated by $\text{B}\square\text{B}$, CBB, and BCB, generating 4, 1, and 2 acceptor sites, respectively. $D = 4c(\text{B}\square\text{B}) + c(\text{CBB}) + 2c(\text{BCB})$.

TABLE 5
Force Constants k (mdyn \AA^{-1}) Calculated from the Resonance Frequency of the Additional Chain (Assumed Models BCB and CCC)

Compound	k (BCB)		k (CCC)	
	calculated	average	calculated	average
$^{10}\text{B}_{6.5}^{12}\text{C}$	4.74		6.11	
$^{11}\text{B}_{6.5}^{12}\text{C}$	4.59	4.73	5.77	6.14
$^{10}\text{B}_{6.5}^{13}\text{C}$	4.85		6.54	
$^{10}\text{B}_{10}^{12}\text{C}$	4.67		6.06	
$^{11}\text{B}_{10}^{12}\text{C}$	4.56	4.69	5.71	6.08
$^{10}\text{B}_{10}^{13}\text{C}$	4.83		6.46	

(ii) The relation $R = c(\text{CBB})/c(\text{CBC})$ is taken from the oscillator strengths of the stretching mode of CBB and CBC chains, respectively (see Fig. 7 in (2)). In this quotient the nonexcludable influence of experimental error in determining the absolute oscillator strengths of the chains is largely eliminated.

(iii) The relation $R_2 = c(\text{BCB})/(c(\text{CBB}) + c(\text{CBC}))$ is taken from the phonon oscillator strengths in Table 2.

(iv) Each rhombohedral unit cell, having any arrangement on the main diagonal, accordingly is $c(\text{B}\square\text{B}) + c(\text{CBB}) + c(\text{CBC}) + c(\text{BCB}) = 1$.

This leads to

$$c(\text{B}\square\text{B}) = \frac{D[(1 - R_2)(1 - R)] - R(1 + 2R_2) - 2R_2}{4[(1 - R_2)(1 - R)] - R(1 + 2R_2) - 2R_2}.$$

For the attribution of CCC arrangements to the separated chain phonon the relations are to be modified as follows:

(i) Since C on the central chain position generates a donor and has no influence on the valence band density of states, one gets $D = 4c(\text{B}\square\text{B}) + c(\text{CBB})$.

(ii) Same as above.

(iii) The relation $R_2 = c(\text{CCC})/(c(\text{CBB}) + c(\text{CBC}))$ is taken from the phonon oscillator strengths in Table 2.

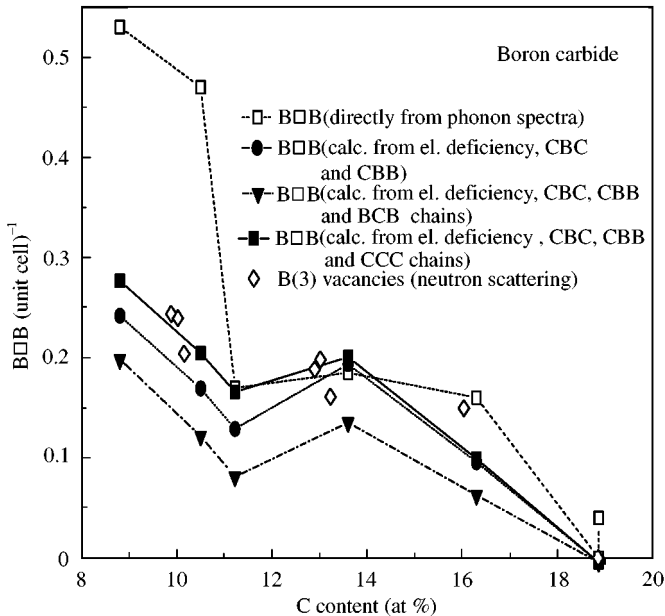


FIG. 3. Concentration of unit cells with $\text{B}\square\text{B}$ arrangements on the trigonal axis, calculated for different assumptions: Additional chain phonon ignored (\bullet), attributed to BCB chains (\blacktriangledown), attributed to CCC chains (\blacksquare). Results directly derived from the absolute phonon oscillator strengths (\square) (1,2,9); B(3) vacancies determined by neutron scattering (\diamond) (16).

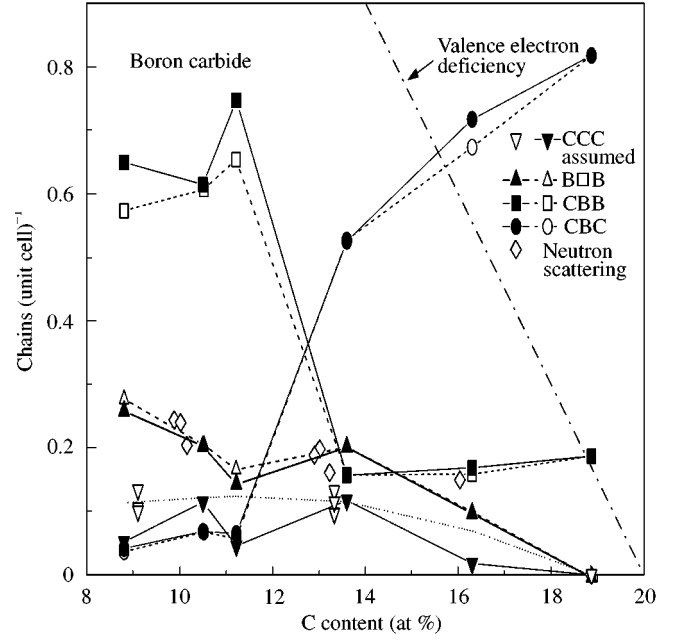


FIG. 4. Concentration of CBC, CBB, CCC chains and $\text{B}\square\text{B}$ arrangements on the trigonal axis per unit cell vs C content. Solid lines connecting filled symbols, results based on the averaged CCC concentrations determined for the isotope-enriched samples presented in this paper (dotted line). Dashed lines connecting open symbols, results based on the measured oscillator strengths of the additional chain phonon obtained from (1,2); (\diamond) B(3) vacancies determined by neutron scattering (16).

(iv) Each rhombohedral unit cell, having any arrangement on the main diagonal, accordingly is $c(\text{B}\square\text{B}) + c(\text{CBB}) + c(\text{CBC}) + c(\text{CCC}) = 1$.

Thus one obtains

$$c(\text{B}\square\text{B}) = \frac{D(1 + R_2)(R + 1) - R}{4(1 + R_2)(R + 1) - R}.$$

In Fig. 3 the concentrations of the $\text{B}\square\text{B}$ arrangements determined from phonon spectroscopy are compared. The results are calculated for different assumptions: The results directly derived from the phonon spectra (1,2) were calculated from the absolute oscillator strengths obtained from the spectra. The deviation in the boron-rich part of the homogeneity range is obviously due to errors caused by nonideal surfaces of the samples, leading to inexact values for the absolute oscillator strengths. This error is largely eliminated when the relations of different oscillator strengths in the same spectrum are used. An excellent agreement is found for the assumption of CCC arrangements.

Accordingly we attribute the additional phonon band to CCC chains. Based on the related equations one determines the concentrations of the different atom arrangements on the trigonal axis (Fig. 4), and using the stoichiometry of the samples, the concentrations of the B_{12} and B_{11}C icosahedra

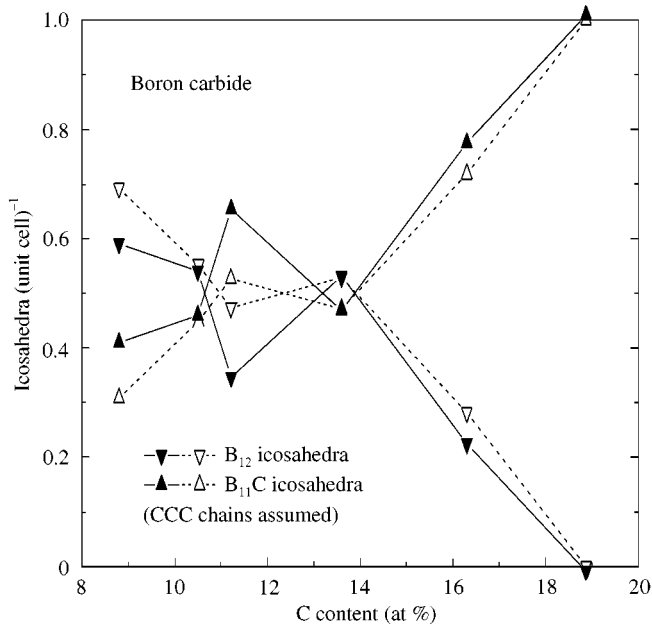


FIG. 5. Concentrations of B_{12} and $B_{11}C$ icosahedra vs C content. Filled symbols, based on the averaged concentration of CCC chains (see Fig. 4); open symbols, based on the measured oscillator strengths of the additional chain phonon obtained from (1,2).

(Fig. 5) as well. The calculations were made (i) for the interpolated concentrations of the additional phonons according to the results in the present paper and for comparison using (ii) the oscillator strengths of the obviously

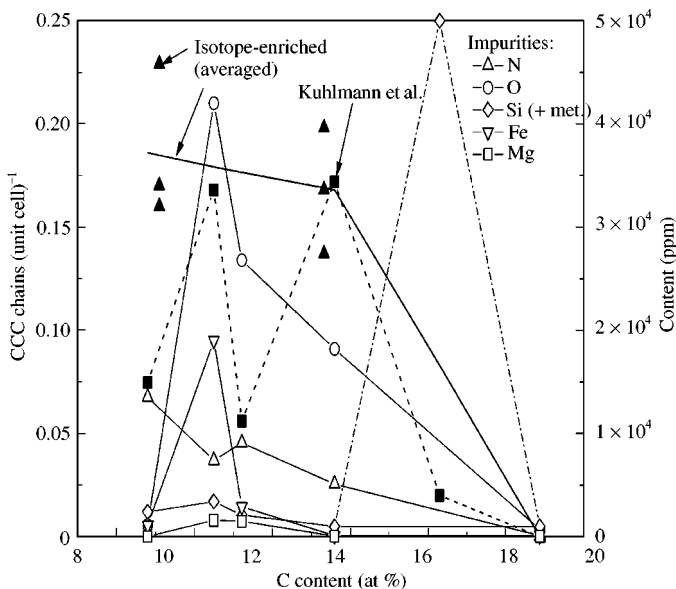


FIG. 6. Concentration of CCC chains vs C content. (\blacktriangle , individual results; solid line, averaged results) this paper; (\blacksquare connected by dashed lines) measured oscillator strengths of the additional chain phonon obtained from (1,2). N, O, Fe, and Mg impurity concentrations of the samples are from (1,2,9); Si is from (20).

same phonons unsystematically appearing in the spectra in (1,2).

The question arises, as to why the additional chain reproducibly occurs in the samples investigated in the present paper but were only accidentally found in former spectra. To check the influence of impurities, in Fig. 6 the CCC concentrations according to the present results and to those in (1,2) are compared with the concentrations of N, O, Fe, and Mg (see Table 1 in (2)) and the Si concentration in doped boron carbide (20). Only a correlation with the Si content is obvious, which is known to form Si_2 chains in otherwise chainless ($B\Box B$) unit cells of boron carbide. Apparently, the Si_2 chains displace CCC chains as well. Since impurities seem not to be responsible, the specific conduction of preparation may be the reason for the occurrence of the CCC chains in boron carbide.

REFERENCES

1. U. Kuhlmann and H. Werheit, *Solid State Commun.* **83**, 849 (1992).
2. U. Kuhlmann, H. Werheit, and K. A. Schwetz, *J. Alloys Compd.* **189**, 249 (1992).
3. R. Schmechel and H. Werheit, *J. Phys. Condens. Matter* **11**, 6803 (1999).
4. D. M. Bylander and L. Kleinman, *Phys. Rev. B* **43**, 1487 (1991).
5. L. Kleinman, in "Boron-Rich Solids, Proceedings 10th International Symposium on Boron, Borides and Related Compounds, Albuquerque, NM, 1990" (D. Emin, T. L. Aselage, A. C. Switendick, B. Morosin, and C. L. Beckel, Eds.), AIP Conf. Proc. 231, p. 13. American Institute of Physics, New York, 1991.
6. U. Kuhlmann, Thesis, University of Duisburg, Germany, 1994.
7. H. Stein, T. Aselage, and D. Emin, in "Boron-Rich Solids, Proceedings 10th International Symposium on Boron, Borides, and Related Compounds, Albuquerque, NM, 1990" (D. Emin, T. L. Aselage, A. C. Switendick, B. Morosin, and C. L. Beckel, Eds.), AIP Conf. Proc. 231, p. 322. American Institute of Physics, New York, 1991.
8. T. L. Aselage, D. R. Tallant, and D. Emin, *Phys. Rev. B* **65**, 3122 (1997).
9. H. Werheit, R. Schmechel, U. Kuhlmann, T. U. Kampen, W. Mönch, and A. Rau, *J. Alloys Compd.* **291**, 28 (1999).
10. H. Binnenbruck and H. Werheit, *Z. Naturforsch. A* **34**, 787 (1979).
11. H. Werheit and H. Haupt, *Z. Naturforsch. A* **42**, 925 (1987).
12. K. Shirai and S. Emura, *J. Phys.: Condens. Matter* **8**, 10,919 (1996).
13. H. Werheit, in "Landolt-Börnstein, Numerical Data and Functional Relationships in Science and Technology," (O. Madelung, Ed.), Vol. 41D, 2000, p. 1.
14. G. Herzberg, "Molecular Spectra and Molecular Structure. II. Infrared and Raman Spectra of Polyatomic Molecules," p. 172. Van Nostrand Reinhold, New York, 1945.
15. J. Waser and J. Pauling, *J. Chem. Phys.* **18**, 747 (1959).
16. R. M. Badger, *J. Chem. Phys.* **2**, 128 (1934); **3**, 710 (1935).
17. B. S. Abbott and C. L. Beckel, in "Boron-Rich Solids, Proceedings 10th International Symposium of Boron, Borides, and Related Compounds, Albuquerque, NM, 1990" (D. Emin, T. L. Aselage, A. C. Switendick, B. Morosin, and C. L. Beckel Eds.), AIP Conf. Proc. 231, p. 344. American Institute of Physics, New York, 1991.
18. G. H. Kwei and B. Morosin, *J. Phys. Chem.* **100**, 8031 (1996).
19. H. Werheit, U. Kuhlmann, M. Laux, and R. Telle, *J. Alloys Compd.* **209**, 181 (1994).